Computational Spectral Display and Capture

Yuqi Li, Hao Zhang, M. Gopi and Aditi Majumder*

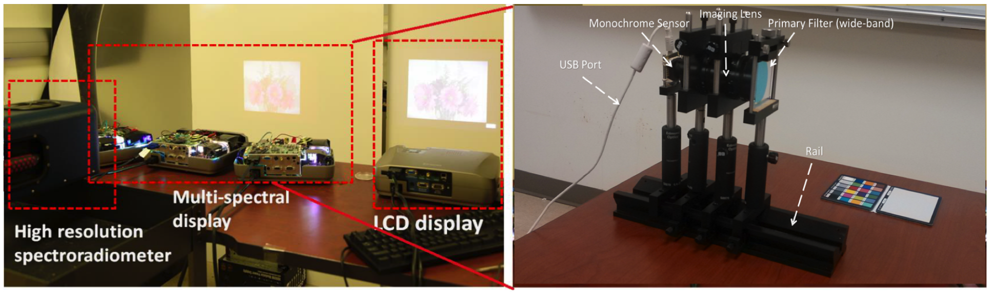

Figure 1: *This shows our multi-spectral display and capture system setups*

Abstract

Spectroscopy, with the current 2D sensors, has been the study of the 4-dimension function $F(x, y, t, l)$ that defines the intensity of light at the sensor location (x, y) at time t and at wavelength l. The goal of video rate spectroscopy is to capture, process, and display this function at reasonable discretized resolutions of each of the parameters x, y, t and l. Spectral imaging till date has been based on three core technologies: filter based, dispersion based or interferometric based. Filter and dispersion based spectral imaging is more general in nature since they try to recover the entire spectrum as opposed to interferometric spectral imaging that targets and captures a specific signature band. An efficient spectral imager can make interferometric spectral imaging redundant. Current spectral imagers use narrow, channel-independent, spectral band primaries that have the fundamental advantage of simple and accurate spectral reconstruction via linear combination of independent spectral channels. However, general spectral imaging today suffers from two fundamental bottlenecks precisely because of the use of narrow band primaries – (a) light inefficiency; (b) inadequate spatial and/or temporal resolution. So, it cannot be used in darker or dynamic environments. Further, in terms of display, use of narrow band primaries may create large color gamut but not a spectrally accurate display. To overcome these limitations, in this paper we explore the usage of wide-band primaries and achieve computational spectral display and capture.

1 Introduction

Although narrow band primaries enable capture and reconstruction of high frequency spectral data, most natural or manmade objects have relatively smooth spectra, in visible, NIR and SWIR ranges [Coulson and Reynolds 1971]. This brings into question the conventional wisdom of light inefficient narrow band filters that deter capturing moving objects. We explore the design, limitations and capabilities of capture and display algorithms and device using a far fewer number of inter-dependent wide-band primaries.

Wide band primaries inherently provide higher light efficiency and can reduce the required number of primaries thereby addressing bottlenecks of light throughput, spatial and temporal resolution. This research aims to present new concepts, techniques and tools in computational dispersion free wide-band spectroscopy which includes (a) selection of inter-dependent primaries to assure maximal information capture; (b) spectral reconstruction and reproduction methods to assure maximal accuracy and quality in capture and illumination respectively; and (c) evaluating the performance and accuracy of this new spectroscopic imaging pipeline with respect to the traditional one that uses narrow band primaries. We show that such a spectroscopic pipeline can achieve video-rate capture, reconstruction and display of spectral data at high spatial resolution.

Spectral data has many applications like detection of oil/mineral; historical manuscript imaging; geographical map creation; monitoring health of crops [Franke and Menz 2007], poultry and meat; sorting good from the bad in food processing and pharmaceutical industry; surveillance against chemical hazards; astronomical imaging; and monitoring unique marine ecosystems, climate and harmful emissions. Current spectral imaging is a niche expensive ($50,000) technology that operates at a low spatial resolution (0.25 Megapixel), a low temporal resolution (a few minutes per frame) and a low dynamic range (1:1000). The proposed video rate light efficient spectral sensor can have a tremendous impact in all of the aforementioned areas. A commodity spectrally accurate illumination working in tandem with such a spectral sensor can open up several new ways for scene parameter reconstruction (e.g. surface reflectance). Finally, a light spectral sensor can augment existing sensor networks enabling fusion of spectral data with regular 3D data for detection and high-resolution monitoring of amorphous objects (e.g. liquids, soot, fire) in a scene contributing tremendously in the domain to scene acquisition and understanding.

1.1 Main Contributions

In this paper, we present a content-independent multi-spectral display via superimposition of wide-band filters on multiple projectors. Similarly the multi-spectral capture is achieved via superimposition of multiple filters over a prototype camera. The main contributions of our work are as follows.

1. We introduce an appropriate guiding rule for selecting multi-spectral primaries. A content-independent primaries selection method is proposed and the chosen set of primaries will be able to achieve high quality of multi-spectral display and capture without significant prior knowledge on the multi-spectral data set.

2. We build a practical multi-spectral image display device by superimposing wide-band filters in the original primaries of three projectors. The experimental results of the prototype demonstrate the higher fidelity of our modified display system over the conventional RGB display

*e-mail:majumder@ics.uci.edu

3. Finally, we build a multi-primary spectral camera. Although for current prototype, the spectrum is captured sequentially. With a well-designed color filters in our following work, the camera should be able to capture scenes in the video rate.

2 Related Works

There have been many recent research works on studying multi-spectral display and capture in the past few years, which aim to achieve accurate color reproduction [Masia et al. 2013]. These techniques are mostly associated with *multi-primary selection*.

Multi-primary based methods aim to apply a set of fixed primaries for modifying the conventional three-primary display system. By superposition of well-chosen filters, the fidelity of color displayed or captured is increased. For multi-spectral display [Roth and Caldwell 2005] uses three band-pass interference mirrors to disperse light, introduces an extra yellow channel to an RGB conventional projector and obtains a 4-primaries front projectors. [Yamaguchi et al. 2001] uses long-pass filters and short-pass filters to modify the RGB channels of two projectors respectively to create a 6-primary display system. Among the recent research, although narrow band primaries have large gamut and are able to reproduce colors that are good enough for CIE standard observes, they fail to project a broadband spectral with great fidelity.

Similarly for multi-spectral recovery, many works have been done to optimize spectral sensitivity of primaries with a regular RGB Bayer color filter [Shen et al. 2014]. Some other works [Park et al. 2007] optimize primaries to minimize the error in spectral recovery. However, they requires strong prior knowledge on the spectral data and needs to know distribution of the spectral functions [López-Álvarez et al. 2007]. Such priors are often domain-specific, these methods cannot apply to arbitrary spectral recovery.

In the following section 3, we will briefly present the required properties for a good set of wide band primaries. In section 4, the multi-spectral display device is succinctly introduced, followed by the multi-spectral capture prototype in section 5.

3 Content-Indepedent Multi-Primary Selection

We evaluate primary combinations using three desired characteristics - completeness of coverage, lower inter-independence and light efficiency. They are explained as follows

Completeness of Coverage: Accurate spectral reproduction requires an almost exact match in the power at every wavelength. Hence, the presence of appropriate transparence rate for every wavelength in our primaries is critical to achieve a good spectral match. Therefore, the spectral sensitivity of our primaries together should cover the entire range of desired wavelength without leaving any obvious "gap".

Low Inter-Primary Dependency: To cover the whole wavelength range using a small number of primaries, wide band filters that have small inter-dependence should be desired. Obviously, if the primaries are all narrow-band their inter-dependency will be low. However, a large number of narrow-band primaries will be required to satisfy the coverage completeness of the entire range. Hence, in our primary selection algorithm [Li et al. 2015], we begin with choosing narrowest band primaries with each cluster, by doing so we can assure a large enough color gamut. If there is any gap in the visible spectrum, we substitute the narrow-band primary with progressively broader band primary from the same cluster until the gap is covered.

Light Efficiency: Low transparency primaries cannot provide a display with sufficient brightness and contrast. Therefore, to assure good quality spectral display or recovery, we prefer light efficient primaries and discard primaries with low intensity from the selecting pool.

[Li et al. 2015] gives more details about our primary selecting algorithm.

4 Multi-primary Multi-spectral Display

In order to create an n primary display using conventional 3-primary projectors, we would need $\lceil \frac{n}{3} \rceil$ projectors. Each primary of a projector is modified by superimposing wide band filters on its original optical path. Replacing original filters on the color wheel of DLP projector or replacing the RGB filters on an LCD projector is one of the possible ways to modify the current primary. However, it is not practically possible because these filters are custom manufactured and well integrated in the optical device. Hence, we instead insert new filters on the illumination path for each channel to create the corresponding primaries. Therefore, the spectral sensitivity of modified projectors will be the product of RGB channel sensitivity and inserted filters sensitivity.

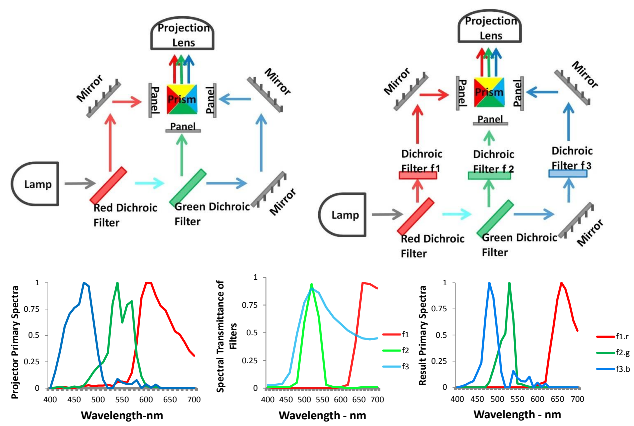

Figure 2: *Modified projector (upper-right) by adding three filters on the optical path of three primaries of an ordinary LCD RGB projector (upper-left). The three existing primaries of the projector (bottom left) is modified by the filters f_1, f_2 and f_3 (bottom middle) to create the modified filters $f_1 \odot r$, $f2 \odot g$ and $f_3 \odot b$ (bottom right).*

5 Multi-Primary Multi-spectral Capture

The spectrum capture is the reverse procedure of display, whose optimal filters can be selected in a similar method. However, for the spectrum display, the captured spectrum is more complex as it is combined with two different components - the light source illumination and the reflectance of object. Hence, the capturing spectrum can be expressed as:

$$S = Pr \tag{1}$$

P is the spectrum of light source and r is the object reflectance. For expression convenience, P is described as a $n \times n$ diagonal matrix

$$P = \begin{bmatrix} P_{\lambda_1} & 0 & \cdots & 0 & 0 \\ 0 & P_{\lambda_2} & 0 & \cdots & 0 \\ \vdots & 0 & P_{\lambda_3} & 0 & \vdots \\ 0 & \cdots & 0 & P_{\lambda_4} & 0 \\ 0 & 0 & \cdots & 0 & P_{\lambda_5} \end{bmatrix} \tag{2}$$

while *r* is a $n \times 1$ vector. As r is the internal property of the object, conventionally it is expressed as an independent variable in the system equation:

$$d = Fr \tag{3}$$

Here d is the sensor response with k different filters, represented as a $k \times 1$ vector, *F* is a $k \times n$ matrix, representing the overall system response:

$$F = (F_f F_{CS})P \tag{4}$$

The whole system response includes several components, the filter spectral sensitivity F_f, camera spectral sensitivity F_{CS} and the previously mentioned light source spectrum. As for the system, there are k different filters and hence F_f is a $k \times n$ matrix. Similar to light source spectrum, camera spectral sensitivity function F_{CS} is also expressed as a diagonal matrix.

Combining equation 3 and 4, the final system equation can be written as:

$$d = (F_f F_{CS})Pr \tag{5}$$

The conventional way to obtain reflectance is by introducing a reconstruction basis. We conduct a similar approach to reconstruct the observed spectrum:

$$Pr = B\sigma \tag{6}$$

B is the reconstructed basis matrix, represented as a $n \times m$ matrix. *m* is a parameter associated with the sparseness of basis function, σ is a $m \times 1$ vector. Each column of *B* represents a basis and σ is the according intensity coefficient. To scope the spectrum reconstruction as optimization problem, an intermediate variable M_s is introduced:

$$M_s = (F_f F_{CS})B \tag{7}$$

Finally, the optimized formula is:

$$argmin_\sigma(|||M_s \cdot \sigma - d|^2 + \alpha|\frac{\partial^2 Pr}{\partial^2 \lambda}|||) \tag{8}$$

The second term imposes a smooth constraint on the observed spectrum and α is a tuning parameter used for penalty control. The smooth term *Pr* can be approximated as:

$$Pr = BM_s^{-1}d \tag{9}$$

The final reconstructed spectrum can be calculated by substituting σ with $\bar{\sigma}_{opt}$ in equation 6

From figure (3) and figure (4), we can see the comparison between reconstructed spectrum using uniformly distributed Gaussian bases and results of the Gaussian bases multiplied by approximate illumination spectrum. It is not difficult to notice, by introducing the illumination heuristic, the reconstructed spectrum can better capture the peak and valley values.

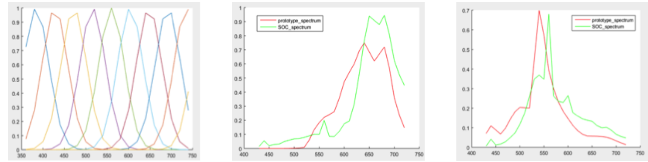

(a) *Gaussian bases* **(b)** *Color green* **(c)** *Color red*

Figure 3: *Reconstructed spectrum of color patches under daylight simulated lamps using Gaussian basis*

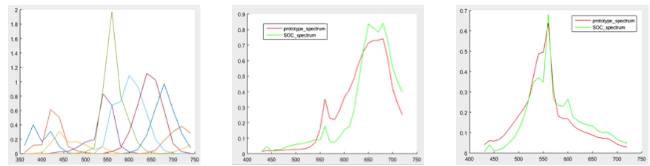

(a) *Ilumination guided bases* **(b)** *Color green* **(c)** *Colorred*

Figure 4: *Reconstructed spectrum of color patches under daylight simulated lamps using Illumination guided bases*

References

BRO, R., AND DE JONG, S. 1997. A fast non-negativity-constrained least squares algorithm. *Journal of chemometrics 11*, 5, 393–401.

CHI, C., YOO, H., AND BEN-EZRA, M. 2010. Multi-spectral imaging by optimized wide band illumination. *International Journal of Computer Vision 86*, 2-3, 140–151.

COULSON, K., AND REYNOLDS, D. W. 1971. The spectral reflectance of natural surfaces. *Journal of Applied Meteorology 10*, 6, 1285–1295.

FRANKE, J., AND MENZ, G. 2007. Multi-temporal wheat disease detection by multi-spectral remote sensing. *Precision Agriculture 8*, 3, 161–172.

JIA, J., BARNARD, K. J., AND HIRAKAWA, K. 2016. Fourier spectral filter array for optimal multispectral imaging. *IEEE Transactions on Image Processing 25*, 4, 1530–1543.

JORDAN, F., AND BACH, F. 2004. Learning spectral clustering. *Adv. Neural Inf. Process. Syst 16*, 305–312.

LI, Y., MAJUMDER, A., LU, D., AND GOPI, M. 2015. Content-independent multi-spectral display using superimposed projections. In *Computer Graphics Forum*, vol. 34, Wiley Online Library, 337–348.

LÓPEZ-ÁLVAREZ, M. A., HERNÁNDEZ-ANDRÉS, J., VALERO, E. M., AND ROMERO, J. 2007. Selecting algorithms, sensors, and linear bases for optimum spectral recovery of skylight. *JOSA A 24*, 4, 942–956.

MASIA, B., WETZSTEIN, G., DIDYK, P., AND GUTIERREZ, D. 2013. A survey on computational displays: Pushing the boundaries of optics, computation, and perception. *Computers & Graphics 37*, 8, 1012–1038.

MONNO, Y., KITAO, T., TANAKA, M., AND OKUTOMI, M. 2012. Optimal spectral sensitivity functions for a single-camera one-shot multispectral imaging system. In *2012 19th IEEE International Conference on Image Processing*, IEEE, 2137–2140.

PARK, J.-I., LEE, M.-H., GROSSBERG, M. D., AND NAYAR, S. K. 2007. Multispectral imaging using multiplexed illumination. In *2007 IEEE 11th International Conference on Computer Vision*, IEEE, 1–8.

RAMANATH, R. 2009. Minimizing observer metamerism in display systems. *Color Research & Application 34*, 5, 391–398.

ROTH, S., AND CALDWELL, W. 2005. 64.4: Four primary color projection display. In *SID Symposium Digest of Technical Papers*, vol. 36, Wiley Online Library, 1818–1821.

SHEN, H.-L., YAO, J.-F., LI, C., DU, X., SHAO, S.-J., AND XIN, J. H. 2014. Channel selection for multispectral color imaging using binary differential evolution. *Applied optics 53*, 4, 634–642.

TERAGAWA, M., YOSHIDA, A., YOSHIYAMA, K., NAKAGAWA, S., TOMIZAWA, K., AND YOSHIDA, Y. 2012. Review paper: Multi-primary-color displays: The latest technologies and their benefits. *Journal of the Society for Information Display 20*, 1, 1–11.

THOMPSON, D. R., MANDRAKE, L., GILMORE, M. S., AND CASTAÑO, R. 2010. Superpixel endmember detection. *IEEE Transactions on Geoscience and Remote Sensing 48*, 11, 4023–4033.

YAMAGUCHI, M., TERAJI, T., OHSAWA, K., UCHIYAMA, T., MOTOMURA, H., MURAKAMI, Y., AND OHYAMA, N. 2001. Color image reproduction based on multispectral and multiprimary imaging: experimental evaluation. In *Electronic Imaging 2002*, International Society for Optics and Photonics, 15–26.